

# Fluxing action of illite and microcline in a triaxial porcelain body

Darunee Wattanasiriwech\*, Suthee Wattanasiriwech

*School of Science, Mah Fah Luang University, Chiang Rai 57100, Thailand*

Received 10 September 2010; received in revised form 10 January 2011; accepted 26 January 2011

Available online 17 February 2011

## Abstract

Comparative studies were made on two types of triaxial porcelain bodies; one used conventional potash feldspar (*STO*) and the other used illite (*ITO*) as the fluxing agents. Scanning electron micrographs showed that densification and mullite formation in the *ITO* body had already occurred at 1000 °C suggesting that there was enough liquid to assist densification and mullite crystal growth. In the *STO* body, mullite crystals started to emerge around 1100 °C, while potash feldspar completely melted around 1200 °C. Full vitrification of the *STO* body required the firing temperature of 1300 °C, which was around 50 °C higher than the *ITO* body. The *ITO* body showed superior strength to the *STO* body at all studied firing temperature ranges and thus was possibly due to (i) a better densification, (ii) a higher amount of interlocking mullite crystals and (iii) the smaller amounts of residual quartz.

© 2011 Elsevier Ltd. All rights reserved.

**Keywords:** Triaxial porcelain; Illite; Microcline; Mullite; Vitrification

## 1. Introduction

The rise in energy demand has accelerated firing technology of ceramic products so that a fast firing scheme is often used. One way forward to achieve such goal, new body recipes have been proposed. Conventional triaxial porcelain body mix contains three main components; clay quartz and feldspar. Vitrification of the body normally starts only when feldspar has melted. It was reported that feldspar melted around 1140–1150 °C without changing its shape until 1200 °C due to its high viscosity.<sup>1,2</sup> In order to achieve complete densification through the viscous flow process of the feldspar, the common firing temperature of the body mix is usually  $\geq 1200$  °C.

During firing, phase transformations and chemical reactions between compositions were observed and reported to affect properties of the final products.<sup>3,4</sup> The final microstructure of the body mainly contains different forms of mullite crystals and undissolved quartz grains dispersed in the glassy matrix. It has been reported that the presence of these crystalline phases were significant to the mechanical behavior of the products.<sup>5</sup> Phase transformation of undissolved quartz grains upon cool-

ing cycle could generate local stresses and microcracks which diminished the flexural strength. In contrast, the presence of mullites, especially the long interlocking-needles was shown to enhance the mechanical properties.<sup>5,7</sup> Dana and Das reported that primary mullite occurred by decomposition of kaolinite crystals, while secondary mullite needles occurred from the reaction between feldspar relict and clay mineral relict.<sup>4</sup> Iqbal and Lee, on the other hand, suggested that primary mullite possibly acted as a seed for the nucleation of secondary mullite.<sup>3</sup> These mullites were distinguished by different morphologies and compositions.<sup>6</sup> Small needle-like structure and interlocking of mullite crystals were proposed to be the key factor for achieving high strength porcelains.<sup>7</sup> Clarification on the formation of mullites will lead to a better body formulation and firing scheme, improved microstructure and hence mechanical properties of ceramic products.

Our previous study on illitic ball clay using X-ray powder diffraction (XRD) and scanning electron microscopy (SEM) showed that vitrification of this clay started around 900 °C and was complete at 1200 °C.<sup>8</sup> Illite is a clay-sized, non-expanding, dioctahedral, aluminous potassium mica-like mineral.<sup>2</sup> Recently illite was defined illite as a “K-deficient mica with an approximate formula of  $K_{0.88}Al_2(Si_{3.2}Al_{0.88}O_{10})OH_2$ .”<sup>9</sup> The existence of liquid phases due to the dissociation of illite crystals in the matrix was thought to enhance the reaction kinetics and densifi-

\* Corresponding author. Tel.: +66 53 916263; fax: +66 53 916776.  
E-mail address: [darunee@mfu.ac.th](mailto:darunee@mfu.ac.th) (D. Wattanasiriwech).

cation rate.<sup>8</sup> Diffusion of potassium ions from the illite crystals to the matrix resulted in the formation of long needle shaped mullite crystals in the illite relict.<sup>8</sup>

In the present study, illite mineral was used as a fluxing agent in ceramic bodies, in parallel with the use of a common fluxing agent, potash feldspar (microcline). Potash feldspar was replaced by illite mineral of the same average size and size distribution at the same weight ratio. Physical properties, phase transformation and vitrification were carefully examined and addressed.

## 2. Experiments

The china clay was from Ranong Province, Thailand. Quartz and potash feldspar (microcline) were also received from domestic commercial suppliers. The illite mineral (Green Shale) was supplied by Ward's Natural Science, Rochester, New York, USA. Chemical analysis of the raw materials was performed using an X-ray fluorescence spectrometer (XRF: Horiba, Japan). The body mix contained 50% china clay, 25% quartz and 25% microcline (STO-) or illite (ITO-). The raw materials were mixed and ground in a ball mill for 6 h and sieved through a 325-mesh stainless steel sieve, then dried in an oven pre-set at 110 °C for 24 h prior to characterization. The sieved clay was then pressed in a stainless steel die at a compaction pressure of 50 MPa into a rectangular bar with the dimensions of 5 mm × 5 mm × 60 mm. Each set of test samples was placed in a muffle furnace and heated to a desired temperature between 900 and 1300 °C in air atmosphere, with a constant heating rate of 5 °C/min. After holding at a maximum temperature for 30 min, the furnace was switched off and the test bars were naturally cooled overnight. In order to clarify the size effect of fluxing agent, potash feldspar and illite mineral was separately ground in a ball mill for 6 h and their average particle size and distribution was measured using a laser diffraction technique (Mastersizer2000, Marlvern, UK). Water absorption values of the fired samples were determined using water immersion technique based on the Archimedes's method while flexural strength values were determined by a three point bending technique using a Universal Testing Machine (Instron 2000, UK). The support span of 80 mm and the crosshead speed of 5 mm/min were chosen for all measurements. The flexural strength was calculated as follows:

$$\sigma = \frac{3}{2} \left[ \frac{FL}{bd^2} \right] \quad (1)$$

where

$\sigma$ : flexural strength (MPa);

$F$ : the load at the fracture point (N);

Table 1  
Chemical analysis of the raw materials.

Oxides	Percent by weight (%)		
	China clay	Illite	Microcline
Al <sub>2</sub> O <sub>3</sub>	36.55	18.53	17.11
SiO <sub>2</sub>	59.28	65.25	69.78
K <sub>2</sub> O	2.15	5.78	10.89
Na <sub>2</sub> O	0.13	–	0.30
MgO	–	2.87	0.12
CaO	0.07	1.19	0.94
TiO <sub>2</sub>	0.08	0.96	0.03
Fe <sub>2</sub> O <sub>3</sub>	1.74	5.27	0.43
Mn <sub>2</sub> O <sub>3</sub>	–	0.04	–
SO <sub>3</sub>	–	0.11	–
P <sub>2</sub> O <sub>5</sub>	–	–	0.38

$L$ : the support span (mm);

$b$  and  $d$ : the width and the thickness of the bar samples (mm), respectively.

These values, averaged from five samples, were reported as a function of firing temperature in order to support the microstructure change.

Phase analysis was performed using XRD and the software X'pert High Score Plus (X'pert Pro MPD, Philips, Netherlands). Microstructure development of fired bars was examined using SEM (LEO 1450 VP). To reveal the crystals on the surface, the fired test bars were subjected to a series of grinding and polishing with 1 μm diamond finish, and etched with 4% hydrofluoric acid (HF) for 2 min prior to microscopy examination.

## 3. Results and discussion

### 3.1. Raw material characterization

The results of chemical analysis as determined by XRF are shown in Table 1. It is noted that the K<sup>+</sup> content in microcline was almost 2 times higher than that in the illite, while Al<sup>3+</sup> and Si<sup>4+</sup> content were only slightly different. Analysis results of the particle size measurement are shown in Table 2. It was shown that illite and feldspar have relatively closed average particle size and distribution. X-ray diffraction analysis (Fig. 1) showed that the clay minerals in china clay were mainly halloysite and kaolinite with some quartz and a small amount of microcline. Illite (Green Shale) contained mainly quartz and illite (K<sub>y</sub>Al<sub>4</sub>Si<sub>8-y</sub>Al<sub>y</sub>O<sub>20</sub>(OH)<sub>4</sub>;  $y = 1.5-2$ ) with a trace of kaolinite. This XRD result suggests that the Fe-ions from the XRF was probably accommodated in the structure of illite. Scanning electron micrographs (Fig. 2) for the china clay revealed obviously elongate crystals of halloysite mixed with the platety crystals

Table 2  
Particle size analysis results obtained from the laser diffraction technique for the ground illite mineral and potash feldspar.

Material	$d(0,1)$ (μm)	$d(0,5)$ (μm)	$d(0,9)$ (μm)	$D(4,3)$ (μm)	$D(3,2)$ (μm)	$S_A$ (m <sup>2</sup> /g)
Illite	1.042	2.782	6.473	3.388	2.099	2.86
Feldspar	1.098	2.676	5.367	3.013	2.102	2.85



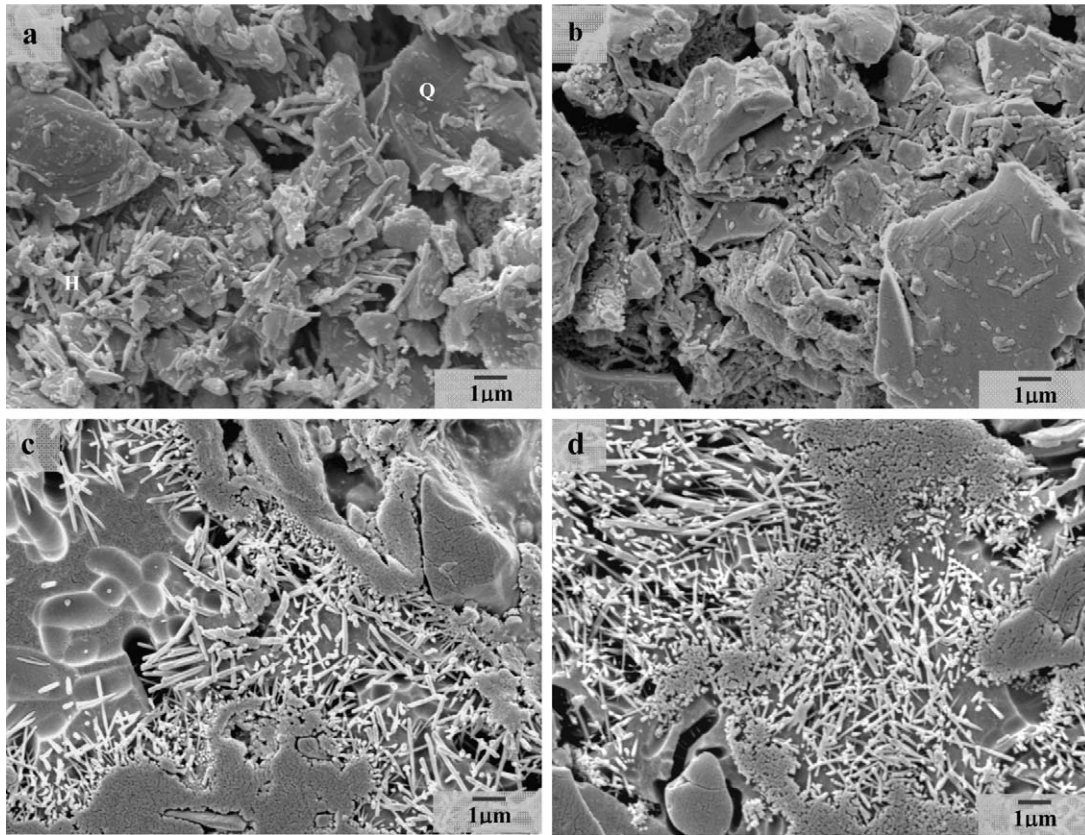


Fig. 5. SEM micrographs showing microstructural changes of the *ST0*-samples fired at (a) 1000 °C, (b) 1100 °C, (c) 1200 °C and (d) 1300 °C.

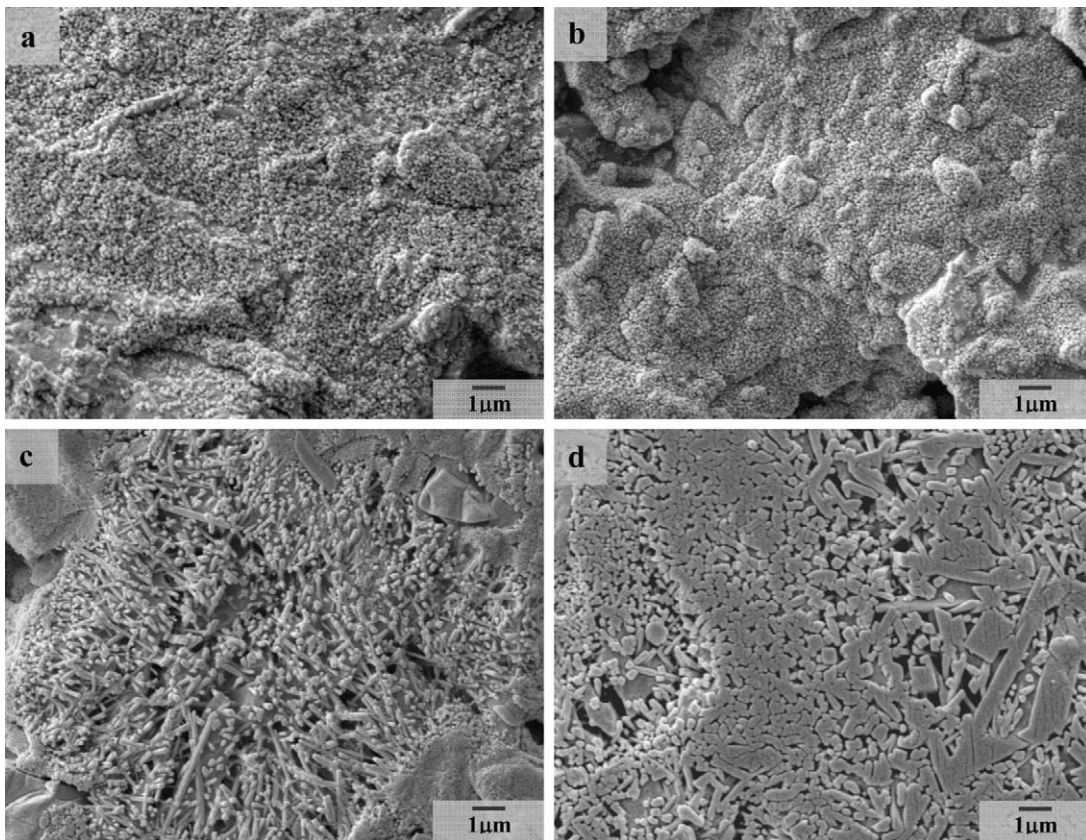


Fig. 6. SEM micrographs showing microstructural change of the *ITO*-samples fired at (a) 1000 °C, (b) 1100 °C, (c) 1200 °C and (d) 1300 °C.

phases after firing at 900 °C. Reflections belonging to halloysite subsided significantly after firing at 1000 °C before finally disappearing at 1100 °C. According to a study of Prodanovi et al., thermochemical reactions of halloysite were relatively similar to those of kaolinite; dehydroxylation around 559 °C into metahalloysite prior to transforming to mullite at 988 °C.<sup>10</sup> Our finding was thus slightly different from that in the reported literature. At 1100 °C, intensity of the microcline reflections was also reduced appreciably while the emergence of mullite peaks could be observed. At 1200–1300 °C reflections belonging to quartz were less intense but still observable. The XRD results for the body containing illite as the main fluxing agent (Fig. 4) showed that illite had transformed into sericite ( $\text{KAl}_2(\text{Si}_3\text{Al})\text{O}_{10}(\text{OH})_2$ ) at 900 °C which is similar to our previous findings.<sup>8</sup> Mössbauer study of pure illite showed that the dehydroxylation actually occurred between 350 and 900 °C whereas this change could not be detected by the XRD.<sup>11</sup> Dehydroxylation of illite was reported to occur via a multi-step mechanism namely a low temperature step and a high temperature step.<sup>12</sup> Mullite peaks started to appear around 1000 °C and continuously grew as the firing temperature was increased. Quartz peaks, in contrast, started to subside around 1100 °C and progressively decreased until 1300 °C. This result suggests that dissolution of quartz may occur to a greater extent in this set of samples.

### 3.3. Microstructural change upon firing

Scanning electron micrographs for the *STO*-samples fired at 1000 °C showed a porous body with halloysite, quartz and some platy shaped particles of dissociated kaolinite (Fig. 5). At 1100 °C, halloysite tubes had substantially disappeared. Increasing the firing temperature to 1200 resulted in vitrification and densification of the body with two mullite morphologies. The short mullite crystals were possibly crystallized from kaolinite relict while the long needed shape mullites were crystallized from feldspar relict. Empty residual glass was also generally observed. At 1300 °C, the amount of long needed shaped mullite increased and the small mullite crystals slightly grew in size.

After firing at 1000 °C, vitrification of the *ITO*-bodies had already started which suggests that there was enough liquid to assist this process and the body was largely covered with nanocrystalline mullite (Fig. 6(a)). This is in good agreement with the XRD result which showed that in the *ITO*-body mullite peaks had already emerged after firing at 1000 °C, which was ~100 °C lower than the *STO*-body. Literature indicates that mullite formed by decomposition of kaolinite occurs around 1100 °C.<sup>3,13</sup> Illite decomposition into mullite and liquid, however, occurred around 900–950 °C<sup>14,15</sup> and 1000 °C.<sup>16</sup> Little change was observed at 1100 °C. When the firing temperature was increased to 1200 °C two morphologies of mullite crystals, cuboidal and elongated, were observed. At 1300 °C, the body was largely covered with mullite crystals with lesser content of empty residual glass. It is noted that the morphology of mullite at this firing temperature was changed to connected lath-like shape i.e. they laterally grew larger with no longer clear distinction in morphologies of the two mullite types. Examination of illite clay

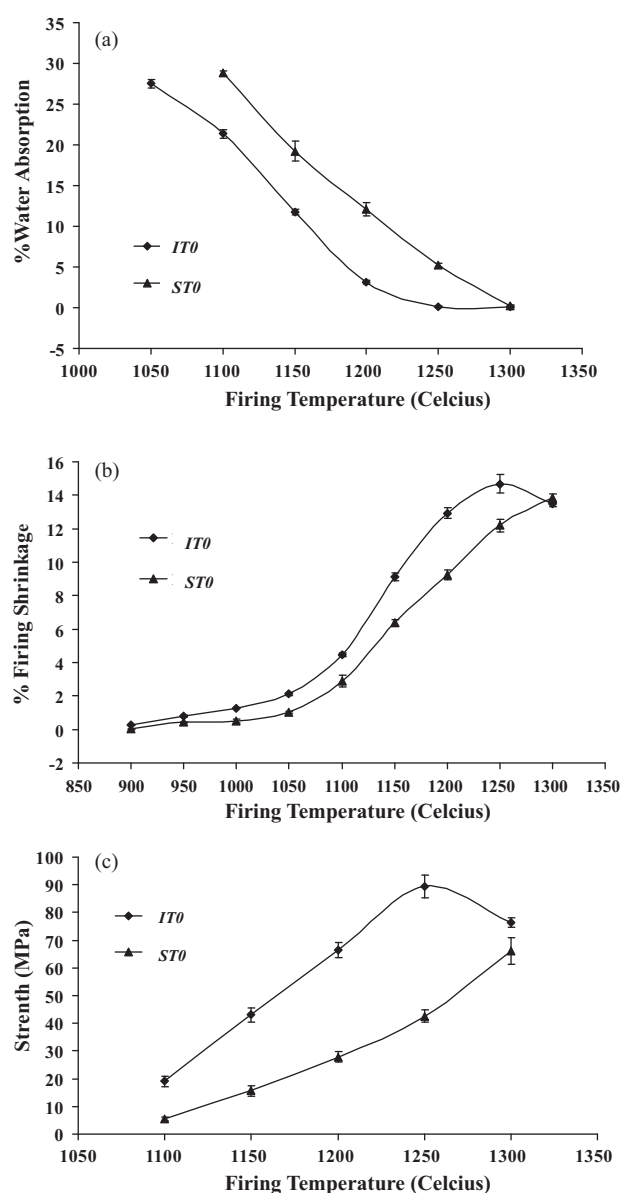


Fig. 7. Variations of 3 key physical characteristics of the standard body (*STO*) and illite modified body (*ITO*) with firing temperature; (a) water absorption, (b) linear shrinkage and (c) flexural strength.

by McConville<sup>17</sup> which was reviewed by Lee et al.<sup>18</sup> indicated that the growth of mullite crystals could be facilitated with the aids of high alkali/ $\text{Fe}_2\text{O}_3$  containing and so fluid silicate liquid. The size of mullite crystals derived from this clay was  $>1 \mu\text{m}$  in diameter while being only  $\sim 100 \text{ nm}$  for those derived from the kaolinite clay. Fe was also reported to act as a mineraliser aiding the growth of mullite crystals in clay.<sup>19</sup> The introduction of iron with the use of illite (see Table 1) as well as the fluidity of the alkaline containing silicate liquid could be the reason that facilitated the growth mullite in our present study.

### 3.4. Physical properties

Key physical properties of both standard (*STO*) and illite modified bodies (*ITO*) are displayed in Fig. 7. Densification of the

*ITO*-bodies was approximately 50–100 °C lower than that of the *STO*-bodies as suggested by both water absorption and linear shrinkage. Earlier densification of the *ITO*-bodies was due to the earlier start of melting compared to feldspar. At 1300 °C, the linear shrinkage of the *ITO*-bodies became regressive without changing the water absorption level due to expansion of trapped gas or so-called “bloating” (SEM picture is not shown here). Bloating was reported to deteriorate strength,<sup>20</sup> in good agreement with the finding here (Fig. 7(c)). It was also noted that the *ITO*-bodies could develop strength with increasing firing temperature more rapidly than the *STO*-bodies possibly due to (i) the higher amount of large interlocking mullite crystals, (ii) the lower porosity and (iii) the lesser content of residual quartz.

The microstructure of a fired triaxial whiteware is a complex features of crystalline phases and pores dispersed in a glassy matrix. As reviewed by Carty and Senapati,<sup>7</sup> strength of a triaxial whiteware increased with increasing mullite content, especially secondary mullite due to its acicular morphology and smaller needle diameter. Pores were regarded as intrinsic flaws which could be the predominant factor deteriorating the strength. In good agreement, a recent study by Montoya et al. showed that improvement of mechanical properties could be associated with an increase of both specimen density and relative content of secondary mullite.<sup>6</sup> In addition, adverse effect of residual quartz to mechanical properties of the fired bodies due to the  $\alpha \rightarrow \beta$  transformation during cooling was addressed.<sup>21</sup> Our XRD results showed that residual quartz amount in the *ITO*-bodies was less than that found in the *STO*-bodies and this could be another factor negatively affecting the fired strength of *STO*-bodies.

#### 4. Conclusions

Illite could be used as a potential fluxing agent in place of potash feldspar although its K<sup>+</sup> content was almost two times lower than that present in feldspar. The illite modified body showed greater densification and thus lower water absorption. The MOR was also improved with lower residual quartz content.

#### Acknowledgements

This project is financially sponsored by Mae Fah Luang University, Thailand and inspired by Mr. Philip C. Robinson. The authors are grateful for both supports. Mrs. Chantane Kwanyun is greatly appreciated for sample preparation.

We thank Professor Kevin D. Hyde for his help in English proof.

#### References

- Kingery WD, Bowen HK, Uhlman DR. *Introduction to ceramics*. 2nd ed. Singapore: John Wiley & Sons; 1991, 535.
- Deer WA, Howie RA, Zussman MA. *Rock forming minerals, volume 3: sheet silicate*. UK: Longmans; 1963. p. 416.
- Iqbal Y, Lee WE. Fired porcelain microstructures revisited. *J Eur Ceram Soc* 1999;**82**(2):3584–4359.
- Dana K, Das SKR. Partial substitution of feldspar by B.F. slag in triaxial porcelain: phase and microstructural evolution. *J Eur Ceram Soc* 2004;**24**:3833–9.
- Kamseu K, Leonelli C, Boccacini DN, Veronesi P, Miselim P, Giancarlo P, et al. Characterisation of porcelain composition using two china clays from Cameroon. *Ceram Int* 2007;**33**:851–7.
- Montoya N, Serrano FJ, Reventós MM, Amigo JM, Alarcón J. Effect of TiO<sub>2</sub> on the mullite formation and mechanical properties of alumina porcelain. *J Eur Ceram Soc* 2010;**30**(4):839–46.
- Carty WM, Senapati U. Porcelain-raw materials, processing, phase evolution, and mechanical behaviour. *J Am Ceram Soc* 1998;**81**:3–20.
- Wattanasiriwech D, Srijan K, Wattanasiriwech S. Vitrification of clay from Malaysia. *Appl Clay Sci* 2009;**43**:57–62.
- Rosenberg PE. The nature, formation and stability of end-member-illite: a hypothesis. *Am Mineral* 2002;**87**:103–7.
- Prodanovi D, Ivkovi B, Radosavljevi S. Kinetics of the dehydroxylation and mullitization processes of the halloysite from the Farbani Potok locality, Serbia. *Appl Clay Sci* 1997;**12**(3):267–74.
- Murad E, Wagner U. Mössbauer study of pure illite and its firing products. *Hyperfine Interact* 1994;**91**:685–8.
- Gualtieri AF, Ferrari S. Kinetics of illite dehydroxylation. *Phys Chem Miner* 2006;**33**:490–501.
- Lee WE, Iqbal Y. Influence of mixing on mullite formation in porcelain. *J Eur Ceram Soc* 2001;**21**:2583–6.
- Grim RE, Bradley WF. Investigation of the effects of heat on the clay minerals illite and montmorillonite. *J Am Ceram Soc* 1940;**23**(8):242–8.
- Khalfaoui A, Kacim S, Hajjaji M. Sintering mechanism and ceramic phases of an illitic-chlorite raw clay. *J Eur Ceram Soc* 2006;**26**(1–2):161–7.
- Aras A. The change of phase composition in kaolinite and illite-rich clay-base ceramic bodies. *Appl Clay Sci* 2004;**24**:257–69.
- McConville CJ. Related microstructural development on firing kaolinite, illite and smectite clays. PhD Thesis, University of Sheffield, UK; 1999.
- Lee WE, Souza GP, McConville CJ, Tavornpanich T, Iqbal Y. Mullite formation in clays and clay-derived vitreous ceramics. *J Eur Ceram Soc* 2008;**28**:465–71.
- Djemai A, Balan E, Morin G, Hernandez G, Labbe JC, Muller JP. Behavior of paramagnetic iron during the thermal transformation of kaolinite. *J Eur Ceram Soc* 2001;**84**:1017–24.
- Wattanasiriwech D, Saengtong C, Wattanasiriwech S. Characterisation of Vieng Kalong clays and relation between physical properties and bloating. *Sci Asia* 2007;**33**:125–30.
- Warshaw S, Seider R. Comparison of strength of triaxial porcelains containing alumina and silica. *J Am Ceram Soc* 1967;**50**(7):337–48.